# 行政院國家科學委員會專題研究計畫　成果報告

## 子計畫三:先進無線通訊系統之關鍵射頻積體電路(I)

計畫類別： 整合型計畫
計畫編號： NSC93-2219-E-009-026-
執行期間： 93 年 08 月 01 日至 94 年 07 月 31 日
執行單位： 國立交通大學電信工程學系(所)

計畫主持人： 孟慶宗

計畫參與人員： 吳宗翰 吳澤宏

報告類型： 完整報告
報告附件： 出席國際會議研究心得報告及發表論文
處理方式： 本計畫可公開查詢

中　華　民　國 94 年 8 月 22 日

行政院國家科學委員會補助專題研究計畫 ■ 成 果 報 告
□期中進度報告

# 先進無線通訊系統之關鍵射頻積體電路(2/3)

# Key RFICs for advanced wireless communication system

計畫類別：□ 個別型計畫　　■ 整合型計畫
計畫編號：NSC93－2219－E－009－026－
執行期間：　93 年　8 月　1 日至　94 年　7 月 31 日

計畫主持人：孟慶宗　國立交通大學電信系
計畫參與人員：吳宗翰 吳澤宏 國立交通大學電信系

成果報告類型(依經費核定清單規定繳交)：■精簡報告　□完整報告

本成果報告包括以下應繳交之附件：
□赴國外出差或研習心得報告一份
□赴大陸地區出差或研習心得報告一份
■出席國際學術會議心得報告及發表之論文各一份
□國際合作研究計畫國外研究報告書一份

處理方式：除產學合作研究計畫、提升產業技術及人才培育研究計畫、列管計畫及下列情形者外，得立即公開查詢
□涉及專利或其他智慧財產權，□一年□二年後可公開查詢

執行單位：國立交通大學電信系

中　華　民　國　　94 年　　7 月　　31 日

# 行政院國家科學委員會專題研究計劃期末報告

## 先進無線通訊系統之關鍵射頻積體電路(2/3)
## Key RFICs for advanced wireless communication system

計畫編號:NSC 93-2219-E-009-026
執行期限:93 年 8 月 1 日至 94 年 7 月 31 日
主持人:孟慶宗　國立交通大學電信系
計畫參與人員: 吳宗翰 吳澤宏 國立交通大學電信系

一、中文摘要

本計劃利用0.35um SiGe BiCMOS製程實現了一個利用LC電流合成器產生單端輸出之5.7GHz升頻微混頻器，混頻器擁有-4dB的轉換增益；一個具鏡像訊號抑制的5.2GHz雙正交四相位降頻器，降頻器擁有1dB的轉換增益與具有47dB的鏡像訊號抑制能力；一個整合集總元件Rat-Race與LC電流合成器的5.2GHz升頻微混頻器。實驗結果與模擬結果大致符合，實驗結果顯示混頻器擁有-1dB的轉換增益。

二、計畫緣由與目的

一般來說，SiGe BJT（鍺化矽雙極性電晶體）技術由於他的截止頻率高且有較好的特性表現，因此通常被用來實現射頻前端電路。單晶射頻積體電路(RFIC)在提供小面積、高重製性、高穩定性及在大量生產時的低價格方面，給射頻技術一個很好的選擇。而砷化鎵晶片雖然價格較高，但在材料的本質上仍勝過矽一大步。但隨著 SiGe 製程技術快速的進步，用此技術來實現前級電路是很方便的，因此將會使得更多人享受行動通訊及無線網路之便利。現在我們在實際應用上已經有以下幾個頻段的需要:GSM (900MHz&1800MHz) ， GPS(1600Mhz) ， DECT(1900Mhz) ， DBS(950-2150MHz)等等，都需要放大器的應用。更重要的是由於無線區域網路(Wireless LAN)的興起，使得在2.4GHz、5.2GHz (汎歐規)及 5.7GHz的頻段出現了應用。因此我們特別選擇這些頻段作為研究重點。

三.研究成果與方法

我們利用了SiGe製程技術，來實現了一個可以在5.7GHz操作之吉伯特升頻微混頻器。我們採用一個被動電感電容合成器使微混頻器的差動輸出轉為單端輸出，同時加倍輸出電流。而微混頻器在本質上就具有寬頻的單端輸入阻抗匹配，因此一個具有單端輸入與單端輸出的吉伯升頻混頻器之運作可以達成。LC電流合成升頻器的電路圖為圖一。我們這裡採用RF Micro Mixer Cell架構，來轉換不平衡的信號為平衡的信號，同時利用高速的BJT來提高工作頻寬及轉換增益。其他的部分再利用LC電流合成的電路，使雙端輸出轉換成單端輸出。一般我們通常會使用主動Balun 作為雙端轉單端電路,不過主動Balun 本身常受到電晶體速度的限制，且線性度也較差。因此我們這個升頻器的RF 輸出端採用LC電流合成的方式將差動輸出訊號轉換成單端輸出。

我們從圖二來看一次LC電流合成器的原理推演。我們將寄生電阻加入後，利用戴維寧與諾頓轉換，將電路

作電流源與電壓源轉換，當電路操作在共振頻率時，串聯的電感與電容會近似短路，而並聯的電感與電容會近似開路，化簡為圖二(d)，在其中定義Q值之後代入Io'，發現當電感Q值夠大時，Io'會等於-Io，而串聯的Cs和Rs與串聯的Ls和Rs則可以利用與Q值之間的關係，化為並聯的Rp、Cp與Lp、Rp，在共振頻率時Cp與Lp又化為開路，所以最後就剩下兩個並聯的Rp與兩倍的Io。因此我們知道要有好的轉換增益，就必須要有高的Rp，要有高的Rp就要有高Q值的電感，但這也是困難的地方。

在複數降頻器電路設計上，為了達到更高的鏡像抑制功能，我們使用雙正交的複數降頻器，由於RF訊號先經過正交的路徑大大減少了中頻鏡像訊號造成的重疊，使得提高了鏡像抑制的能力。雙正交相位複數降頻器電路圖的電路圖為圖三。包含了四個混頻器所組成的雙正交複數降頻器、去除鏡像訊號的RC-CR多相位濾波器、LO及RF的正交相位產生器，以及RF輸入端的被動差動訊號產生器。由於RF訊號先經過正交的路徑大大減少了中頻鏡像訊號造成的重疊，使得提高了鏡像抑制的能力。在圖四(a)中利用重疊原理，可以看出相位為0º 的輸入訊號在等效上看到一個CR高通濾波器，而相位為90º 的輸入訊號等效上看到一個RC低通濾波器。在極點頻率時，其相位分別落後45º(+45º)及超前45º (-45º)。因而相位為0º的輸入訊號落後45º成為45º，而相位為90º的輸入訊號超前45º成為45º，即輸出的訊號同相。而在圖四(b)中利用相同的重疊原理，分別輸入0º、270º 的訊號，因而相位為0º的輸入訊號落後為45º，但相位為270º的輸入訊號超前45º成為225º，因而輸出的訊號相差180º，此時無訊號輸出。由以上我們可得知，對於一個逆時間方向的正頻率訊號可以順利到達輸出端，而對於一個逆時間方向的負頻率訊號則在到達輸出端前被相減。由於LO輸入部份需要I/Q的訊號，因而我們一樣可以利用RC-CR的多相位濾波器來產生。如圖五所示，一差動的訊號等效上可以看成正頻率與負頻率的組合，由於多相位濾波器可以分辨正負頻率的差別，因此一差動訊號可經由多相位濾波器濾除負頻率項後產生所需的正交訊號。我們這裡使用吉伯特混頻器，如圖六。再加上共集極電晶體以防止後面的多相位濾波器所造成的負載效應。最後再使用一個簡單的差動放大器來當作中頻輸出級，如圖七，將中頻信號合成以方便量測。

而整合集總元件Rat-Race與LC電流合成器的升頻微混頻器電路如圖八，本電路大部分的架構都與前一個LC電流合成器相似，但是我們修改了RF輸入級為更平衡的結構，同時將產生LO差動訊號所需的Rat-race以集總元件的方式時限內建在晶片裡，並且修改輸出級由原先的LC低通濾波器換為CC-CC輸出級。如圖八，LO 信號連接到一個集總元件組成的Rat-race。因為在RF的量測環境中，通常有很多用來連接探針與儀器的訊號線與轉接器，而這些外部的連接多是造成輸入訊號不平衡的原因。而現在的製程技術已微小到可以在這樣的高頻下，讓集總Rat-race整合到晶片中，所以最直接的作法便是將Rat-race作進晶片裡。集總元件Rat-race 電路如圖九所示。在此升頻器的輸出部份，一樣使用電流合成器輸出單端電流，為了使電流合成器不受外部的電路影響，在輸出端加上一個CC-CC的緩衝級隔離外部的電路，如圖十所示。

我們可以發現輸出電壓緩衝級實際上是提供功率增益。更進一步地說，由電壓緩衝級得到的功率增益要比我們在前一個電路裡所採用的純電抗匹配來的好。LC電流合成器電路的等效單端輸出電路如圖十一所示，將

諾頓等效電路轉換為戴維寧等效電路是為了討論傳遞到負載的功率。如圖十一(b)，如果使用一個電抗匹配網路來匹配LC電流合成器輸出阻抗至50歐姆，最大傳遞到負載的功率同時達到共軛狀態時，可以用下式來表示：

$$P_{\text{L Passive Matching}} = \frac{\left|I_{sig}\right|^2 R_{sig}}{4}$$

而如果使用的是主動輸出電壓緩衝級，我們可由圖十一(c)來說明。電壓緩衝級的輸出阻抗為50歐姆，而輸入阻抗則遠大於LC電流合成器的阻抗，所以當使用主動輸出電壓緩衝級時，傳遞到負載的功率可以表示為：

$$P_{\text{L Active Buffer}} = \frac{\left|V_{sig}\right|^2}{4Z_0} = \frac{{I_{sig}}^2 \bullet {R_{sig}}^2}{4Z_0}$$

比較兩式，使用主動輸出級之傳遞到負載的功率較高。因此，功率提升度可以由兩式的比值來表示：

$$\frac{P_{\text{L Active Buffer}}}{P_{\text{L Passive Matching}}} = \frac{\dfrac{\left|I_{sig}\right|^2 \bullet {R_{sig}}^2}{4Z_0}}{\dfrac{\left|I_{sig}\right|^2 \bullet R_{sig}}{4}} = \frac{R_{sig}}{Z_0} = \frac{R_P}{2Z_0}$$

在類比電路設計中，輸出緩衝級不提供電壓增益，然而共集極輸出緩衝級能提供功率增益。事實上，功率增益是由主動輸出緩衝級而來，而主動輸出緩衝級藉由電流信號來提供額外的功率而不是藉由電壓信號。值得注意的是主動輸出緩衝級的輸入阻抗與電流合成器的輸出阻抗並非互相共軛。這個設計方法與微波放大器電路的電抗匹配原理相當不同。這裡的設計概念不只符合類比電路設計概念，也同時讓我們清楚知道由類比IC設計裡的電壓電流增益，轉換到RFIC設計裡的功率增益。

四.結果與討論

圖十二為LC電流合成升頻器電路晶片照片。而圖十三顯示LC電流合成升頻器轉換增益對LO power的量測圖形。當LO power為3dBm時，轉換增益峰值約為-4dBm。當LO power從-10dBm增加到3dBm時，轉換增益隨之由-6dB增加到-4dB。換句話說，混頻器核心只需要低功率的本地震盪源，並且對理想的轉換增益具有寬的LO power範圍。圖十四顯示RF輸出反射損耗在5.7GHz時約為-25dB。RF輸出阻抗匹配我們是利用一個LC低通濾波器來作的。在我們的電路設計裡，操作頻率為5.7GHz而量測結果顯示出輸出反射損耗正好在5.7GHz的位置有個凹口，顯示我們的阻抗匹配作得很好。圖十五可以得知這個LC電流合成器的功率特性表現。實驗的數據顯示OP1dB為-9.5dBm，OIP3為-1.5dBm，因此我們可以知道這個架構的線性度很不錯。

圖十六為雙正交相位複數降頻器晶片照片。我們從量測結果圖十七可以發現，當降頻混頻器的RF=5.2GHz、LO=5.17GHz，LO power為0dBm時，電路具有1dB的轉換增益。從圖中可以發現，當LO power從0dBm增加到10dBm時，轉換增益仍維持在1dB左右。換句話說，混頻器所需要的LO power不大，同時具備寬的LO power變化範圍來達成我們所要求的轉換增益。因此我們的吉伯特混頻器核心具有低LO power與寬LO power變化範圍的兩個優點。由圖十八中可以看到在15MHz到45MHz的IF頻段，IRR大於47dB。

圖十九為整合集總元件Rat-Race與LC電流合成升頻器電路晶片照片。圖二十顯示轉換增益對LO power的量測圖形。當LO power為0dBm時，轉換增益峰值約為-1dBm。當LO power從-6dBm增加到5dBm時，轉換增益維持在-1dB。圖二十一為電路的IF埠與RF埠反射損耗。RF輸出反射損耗從0.1GHz一直到20GHz都在-13.5dB以下。微混頻器具有寬的輸入阻抗匹配頻寬，所以在圖中可以看到從低頻一

直到20GHz，IF的輸入阻抗匹配約在-10dB以下。圖二十二可以得知這個LC電流合成器的功率特性表現。實驗的數據顯示OP1dB為-10dBm，OIP3為6dBm，因此我們可以知道這個架構的線性度非常不錯，而這個電路的高線性度應該是直接來自因使用了被動電感電容電流合成器來當作負載的緣故。

五.計畫成果與自評

研究內容和原計畫完全相符，達成了預期目標情況，已發表在相關學術期刊及研討會中。

六.參考文獻


[1] B. Gilbert, “The MICROMIXER: A highly linear variant of the Gilbert mixer using a bisymmetric Class-AB input stage,” IEEE J. Solid-State Circuits, Vol. 32, pp. 1412-1423, Sept. 1997.

[2] J. Durec and E. Main, “A linear class AB single-ended to differential transconverter suitable for RF circuits,” IEEE MTT-S Dig., pp. 1071-1074, 1996.

[3] C. C. Meng, S. K. Hsu, A. S. Peng, S. Y. Wen and G. W. Huang, “A fully integrated 5.2 GHz GaInP/GaAs HBT upconversion micromixer with output LC current combiner and oscillator”, IEEE MTT-S international microwave symposium. pp. A205-A208, 2003.

[4] C. C. Meng, S. S. Lu, M. H. Chiang, and H. C. Chen, “DC to 8 GHz 11 dB gain Gilbert micromixer using GaInP/GaAs HBT technology”, Electronics Letters, pp.637-638, April 2003.

[5] C. C. Meng, S. K. Xu, T. H. Wu, M. H. Chao and G. W. Huang, “A high isolation CMFB downconversion micromixer using 0.18 um deep n-well CMOS technology”, IEEE MTT-S international microwave symposium. pp. A105-A108, 2003.

[6] F. Behbahani, Y. Kishigami, J. Leete, and A. Abidi, “CMOS Mixers and Polyphase Filters for Large Image Rejection,” IEEE Journal of solid-state circuits, VOL. 36, NO. 6, JUNE 2001.

[7] J. Crols and M. Steyaert, “Fully Integrated 900 MHz CMOS Double Quadrature Downconverter,” Proc. ISSCC, Session 8.1, San Francisco, Feb. 1995.

[8] J. Crols and M. Steyaert, “A Single-Chip 900 MHz CMOS Receiver Front-End with a High Performance Low-IF Topology,” IEEE J. of Solid-State Circuits, vol. 30, no. 12, pp. 1483-1492, Dec. 1995.

[9] M. Steyaert, M. Borremans, J. Janssens, B. D. Muer, N. Itoh, J. Craninckx, J. Crols, E. Morifuji, H. S. Momose and W. Sansen, “A single-chip CMOS transceiver for DCS-1800 wireless communications” Proc. ISSCC, San Francisco, Feb. 1998.


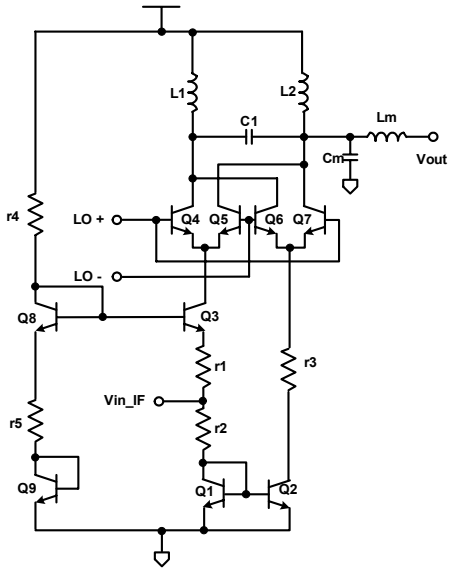


圖一　LC 電流合成升頻器電路

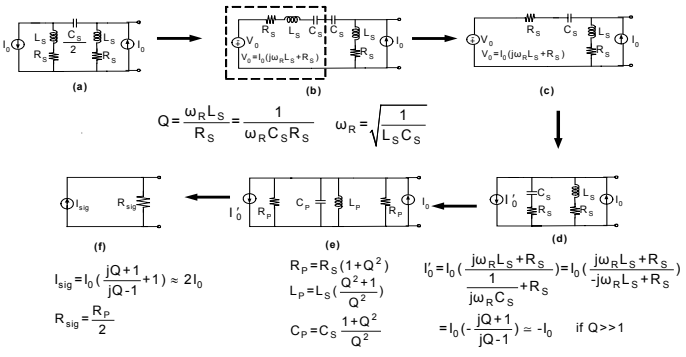


圖二　加入寄生電阻之電流合成器等效轉換圖

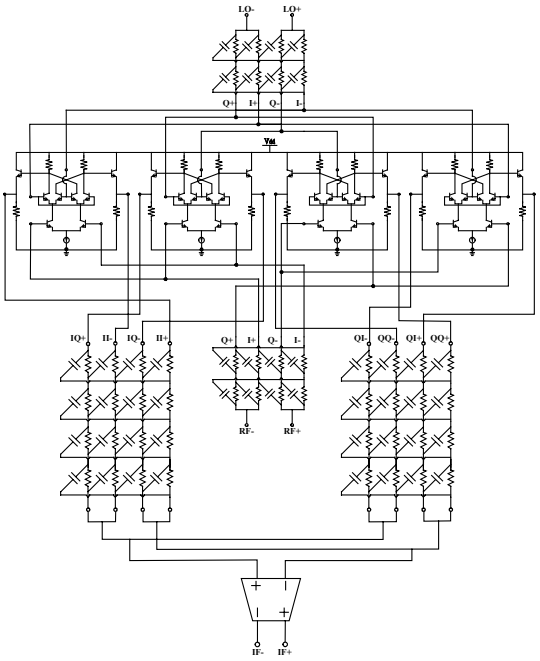


圖三　雙正交相位複數降頻器電路圖

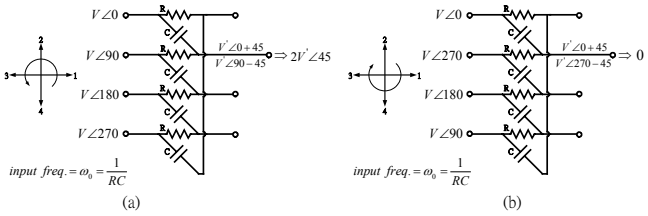


圖四 RC-CR 多相位濾波器(a)正頻率

(b)負頻率選擇

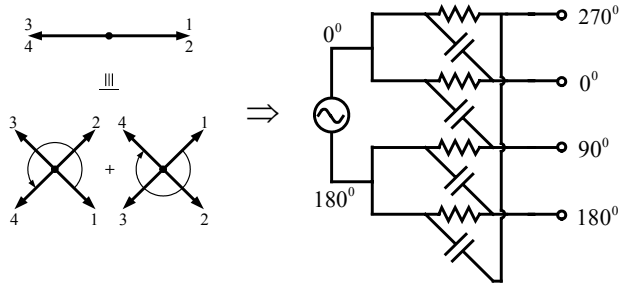


圖五 正交訊號產生器

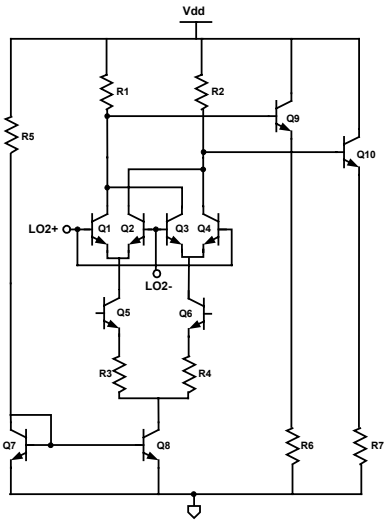


圖六 吉伯特混頻器

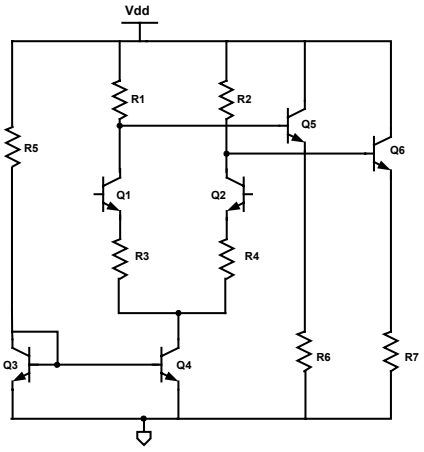


圖七 中頻輸出級

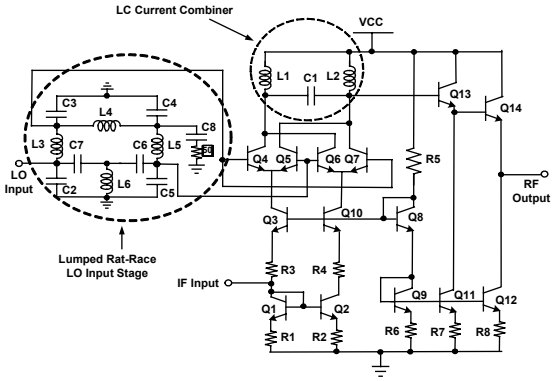


圖八　內建集總Rat-race之LC電流合成升頻器電路

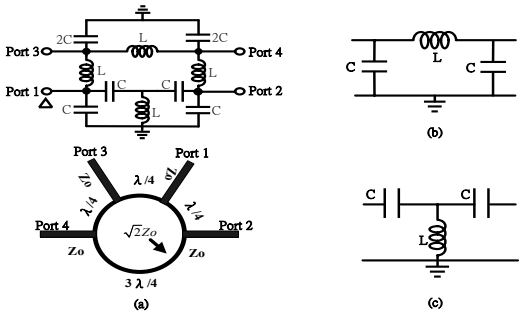


圖九 集總 Rat-Race

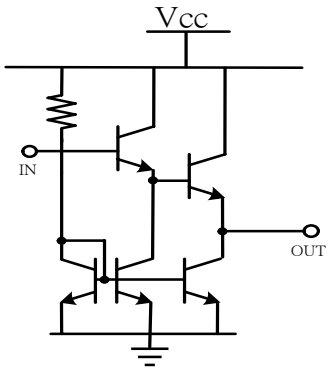


圖十 CC-CC 輸出級

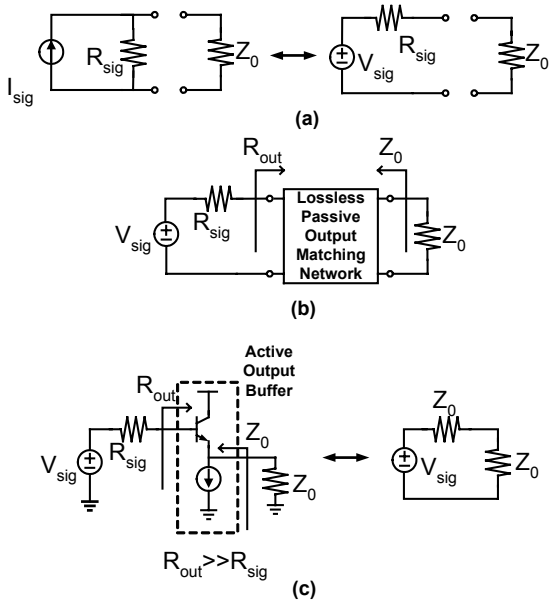


圖十一 LC 電流合成級與射頻輸出級的輸出功率轉換

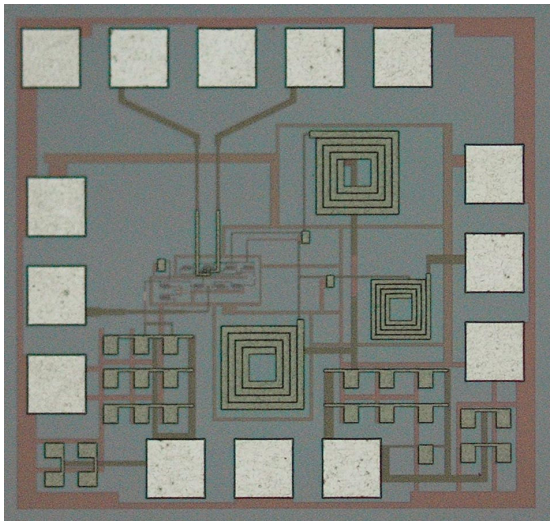

圖十二 LC 電流合成升頻器晶片照片

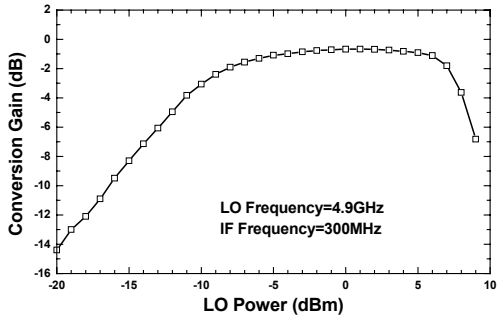


圖十三 LC 電流合成升頻器電路轉換增益對 LO 功率量測結果

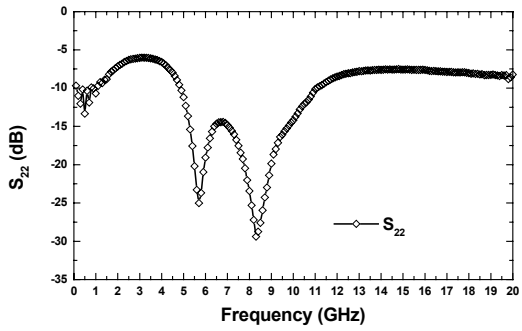


圖十四 LC 電流合成升頻器電路 S22 量測結果

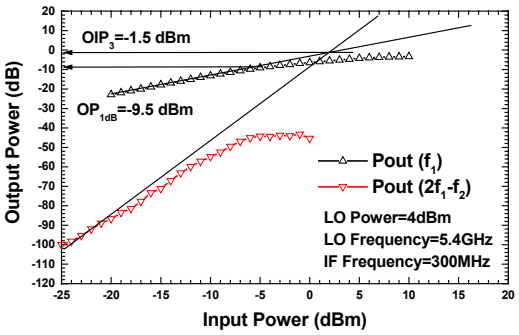


圖十五　LC 電流合成升頻器電路功率特性量測結果

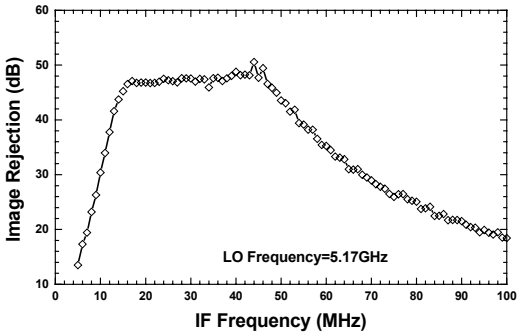


圖十八　雙正交相位複數降頻器電路 IRR 量測結果

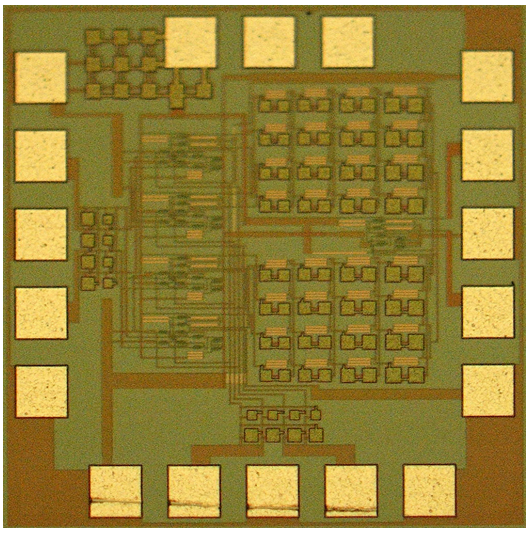

圖十六　雙正交相位複數降頻器晶片照片

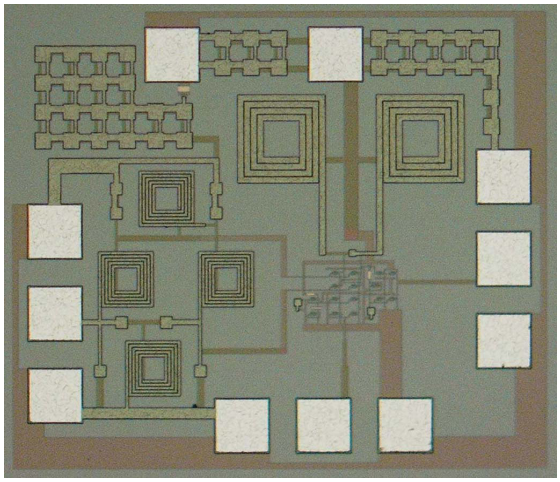

圖十九　內建集總 Rat-race 之 LC 電流合成升頻器晶片照片

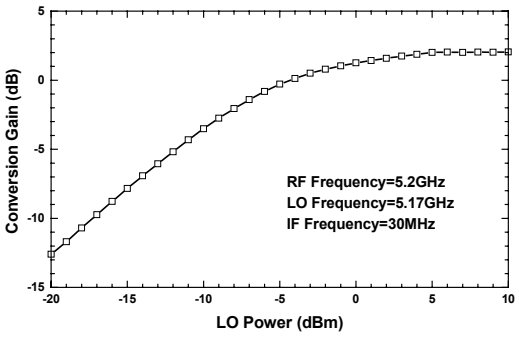


圖十七　雙正交相位複數降頻器電路轉換增益對 LO 功率量測結果

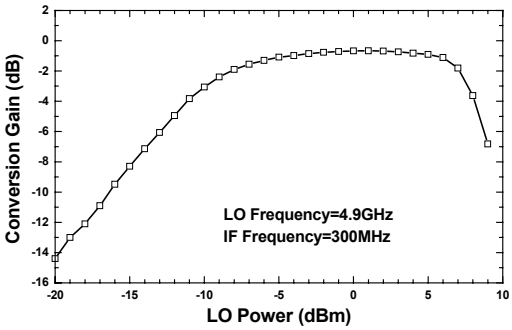


圖二十　內建集總 Rat-race 之 LC 電流合成升頻器電路轉換增益對 LO 功率量測結果

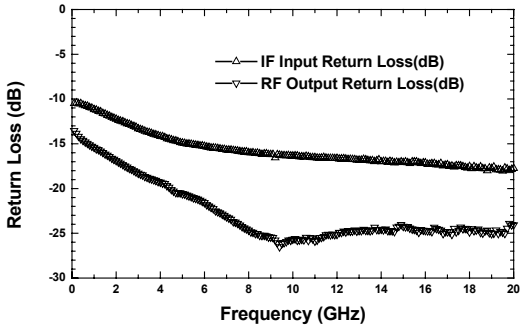


圖二十一　內建集總 Rat-race 之 LC 電流合成升頻器電路 S 參數量測結果

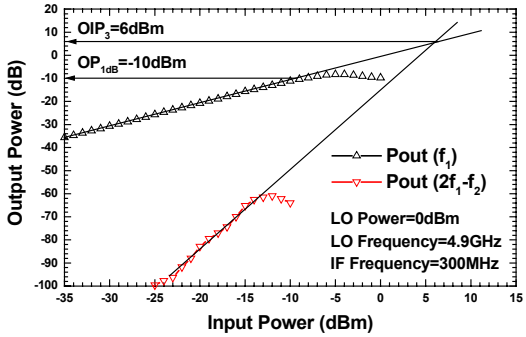


圖二十二　內建集總 Rat-race 之 LC 電流合成升頻器電路功率特性量測結果

發表之論文

Tzung-Han Wu, Chinchun Meng, Tse-Hung Wu and Guo-Wei Huang “A 5.7 GHz 0.35 um SiGe HBT Upconversion Micromixer with a Matched Single-ended Passive Current Combiner Output”, European Microwave Conference - European gallium arsenide and other semiconductors application symposium (GAAS 2004), Amsterdam, Netherlands, October 11-15, 2004, pp.323~326

Tzung-Han Wu, Chinchun Meng, Tse-Hung Wu and Guo-Wei Huang, “A Fully Integrated 5.2 GHz SiGe HBT Upconversion Micromixer Using Lumped Balun and LC Current Combiner”, IEEE 2005 International Microwave Symposium, Long Beach, California, June 12-17, 2005

Tzung-Han Wu, Chinchun Meng, Tse-Hung Wu, and Guo-Wei Huang, “A 5.7 GHz Gilbert Upconversion Mixer with an LC Current Combiner Output Using 0.35 um SiGe HBT Technology”, IEICE Trans. Electron., Vol.E88-C, No.6, pp.1267-1270 June 2005

# A Fully Integrated 5.2 GHz Double Quadrature Image Rejection Gilbert Downconverter Using 0.35 μm SiGe HBT Technology

Chinchun Meng[1], Tzung-Han Wu[1], Tse-Hung Wu[1] and Guo-Wei Huang[2]

[1]Department of Communication Engineering, National Chiao Tung University, Hsin-Chu, Taiwan, R.O.C.
[2]National Nano Device Laboratories, Hsin-Chu, Taiwan, R.O.C.

*Abstract* — **A 5.2 GHz 1 dB conversion gain, $IP_{1dB}$= -19 dBm and $IIP_3$= -9 dBm double quadrature Gilbert downconversion mixer with polyphase filters is demonstrated by using 0.35 μm SiGe HBT technology. The image rejection ratio is better than 47 dB when LO=5.17 GHz and IF is in the range of 15 MHz to 45 MHz. The Gilbert downconverter has four- stage RC-CR IF polyphase filters for image rejection. Polyphase filters are also used to generate LO and RF quadarture signals around 5 GHz in the double quadrature downconverter.**

## I. Introduction

Recently, integrated polyphase filters and the double quadrature configuration have been used in the low IF topology in CMOS technology [1], [2], [3], [4]. A low-IF receiver topology consists of RF IQ paths and the integrated polyphase filters to eliminate the off–chip noise filters and IF filters for image rejection. When a large image rejection is required such as in a low-IF topology, a double quadrature downconversion arrangement is better than a single quadrature downconversion arrangement because the double quadrature downconversion has less quadrature accuracy requirement. The LO and RF quadrature signal generation can be implemented by the polyphase filters in a double quadrature downconverter. An HBT transistor has better device matching property than a MOS device. Thus, it is desirable to have a high image rejection double quadrature Gilbert downconverter with polyphase filters in the SiGe HBT technology. The fabricated SiGe HBT double quadrature Gilbert downconversion mixer with polyphase filters has 1 dB conversion gain, $IP_{1dB}$= -19 dBm and $IIP_3$= -9 dBm at 5.2 GHz. The image rejection ratio is better than 47 dB when LO=5.17 GHz and IF is in the range of 15 MHz to 45 MHz. The supply voltage is 2.7 V and current consumption is 10 mA.

## II. Circuit Design

Figure 1 illustrates the system block diagram of a double quadrature downconverter with polyphase filters. Differential RF and differential LO signals are fed externally and two polyphase filters are used to generate LO and RF differential quadrature signals.

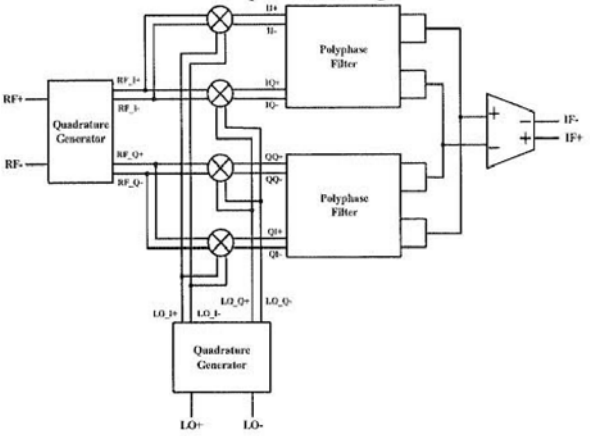


Figure 1 Block diagram of a double quadrature downconversion mixer with polyphase filters.

Four Gilbert multipliers are used in figure 1 to form a complex mixer. Thus, the desired signal and the image signal will appear in different rotational sequences at the output of the complex mixer as explained in reference [1]. Then the image signal will be filtered away by the IF polyphase filters and the desired signal will pass directly through the IF stage. The differential quadrature IF signals following the IF polyphase filter are combined into differential signals by properly shorting the differential quadrature IF signals.

Figure 2 illustrates the detailed schematic of the image rejection downconverter. Two-stage polyphase filters are used to generate both LO and RF differential quadrature signals from their differential counterparts. A conventional Gilbert cell with a differential common collector output buffer is used as the multiplier. The image rejection is performed by using two four-stage RC-CR polyphase filters. The differential quadrature IF signals are combined into differential signals by properly shorting the differential quadrature IF signals and a differential

buffer amplifier is also included in the IF final stage as illustrated in figure 2.

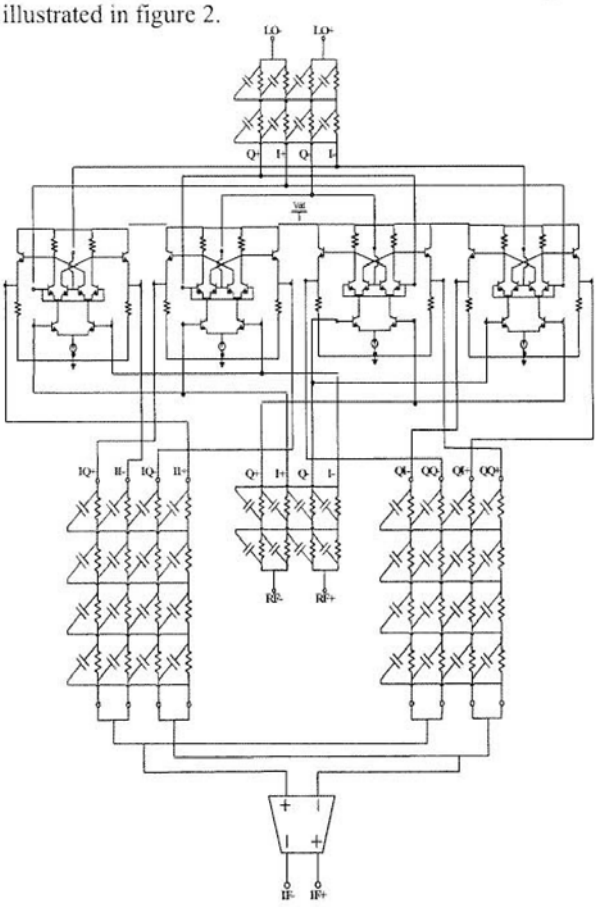

Figure 2 Circuit schematic of a SiGe HBT double quadrature downconversion mixer with polyphase filters.

## III. Experimental Results and Discussions

The die photograph of a SiGe HBT double quadrature downconverter mixer with polyphase filters is shown in figure 3. The die size is 1x1 $mm^2$. The SiGe HBT device used in this work has $BV_{CEO}$=3.8 V and peak $f_t$ around 49 GHz. On-wafer RF measurements are performed because the fabricated circuit in figure 3 has a balanced GSGSG RF input on the left side of the chip, a GSGSG IF output on the right side and a balanced GSGSG LO input on the bottom side. Two ratrace couplers are used to convert the single-ended signals to differential signals. One ratrace for RF signals is centered at 5.2 GHz and the other ratrace for LO signals is center at 5.17 GHz. The phase imbalance is less than 1° and the magnitude imbalance of the ratrace is less than 0.03 dB in 0.1 GHz bandwidth. Bias tees are inserted between the retrace and the signal generator to provide dc bias for transistors at RF and LO ports.

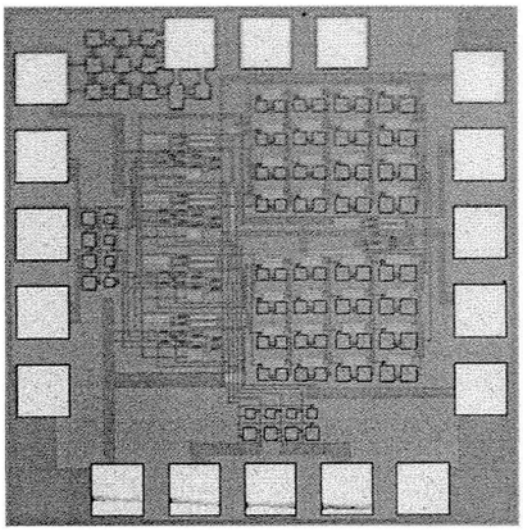

Figure 3 Photograph of a SiGe HBT double quadrature downconverter with poly phase filters

The conversion gain is 1 dB for 0 dBm LO pumping power when LO=5.17 GHz and RF=5.2 GHz. The conversion gain varies within 1 dB while LO power changes from 0 dBm to 10 dBm as shown in figure 4. In other words, the required LO power is small and there exists a wide range of LO power for optimum conversion gain. A Gilbert mixer core implemented with bipolar type technology needs a small local oscillator power and has a wide range of LO power for optimum conversion gain. When LO power equals to 0 dBm, the LO-to-IF isolation measurement results are illustrated in figure 5. 48 dB LO-IF isolations are achieved in the downconverter when LO frequency is around 5.2 GHz. The circuit has more than 49 dB RF-IF isolation as shown in the figure 6 when LO frequency is at 5.17 GHz and power equals to 0 dBm.

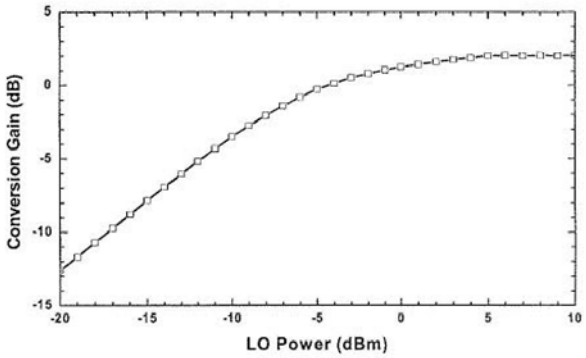


Figure 4 Conversion gain as a function of LO power of the SiGe HBT double quadrature downconverter with poly phase filters.

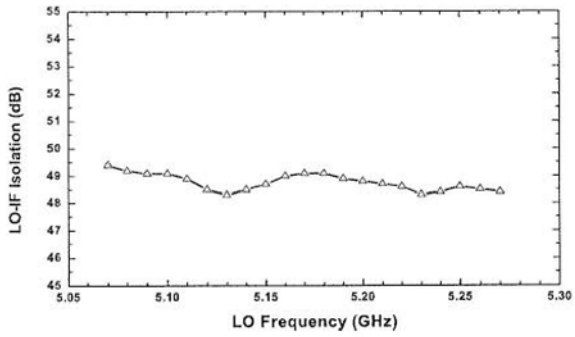


Figure 5 Measured LO-IF isolation of the SiGe HBT double quadrature downconverter with poly phase filters.

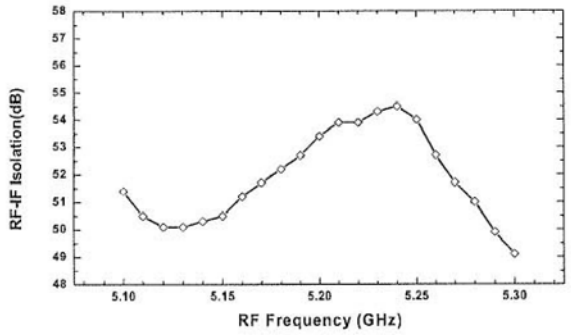


Figure 6 Measured RF-IF isolation of the SiGe HBT double quadrature downconverter with poly phase filters.

The one-tone and two-tone power performance is shown in figure 7 and figure 8, respectively. The fabricated SiGe HBT double quadrature Gilbert downconversion mixer with polyphase filters has 1 dB conversion gain, $IP_{1dB}$= -19 dBm and $IIP_3$= -9 dBm. All the power measurements are performed when RF=5.2 GHz and LO=5.17 GHz at 0 dBm.

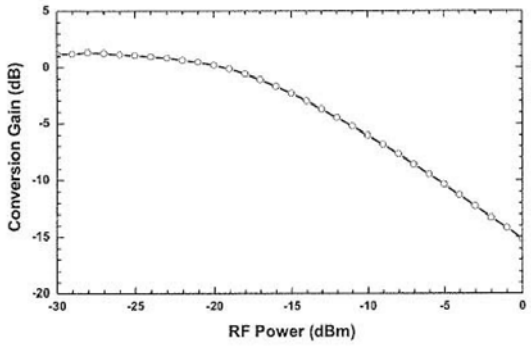


Figure 7 One tone power measurements of the SiGe HBT double quadrature downconverter with poly phase filters.

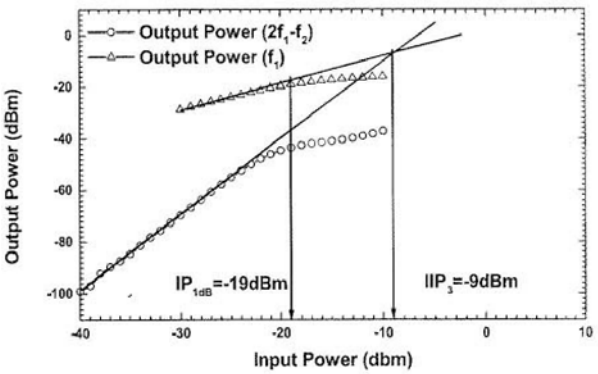


Figure 8 One tone and two tone power measurements of the SiGe HBT double quadrature downconverter with poly phase filters.

Figure 9 illustrates the conversion gain as a function of positive IF frequency and negative IF frequency when LO=5.17 GHz and 0 dBm. The IF frequency is positive if the RF frequency is larger than the LO frequency. Otherwise, the IF frequency is negative. The axis for negative IF frequency is folded back to highlight the comparison with positive frequency in figure 9. The conversion gain is about 1 dB for 15 to 45 MHz positive IF frequency and is -46 dB for 15 to 45 MHz negative IF frequency. The image rejection ratio defined as the ratio between positive IF conversion gain and negative IF conversion gain is plotted in figure 10. Image rejection ratios are better than 47 dB for 15 to 45 MHz IF frequencies.

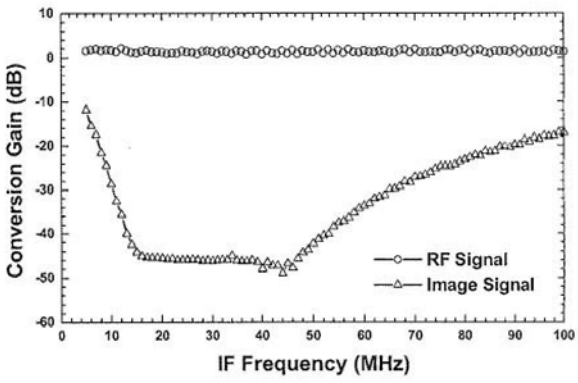


Figure 9 Conversion gain as a function of IF frequency for the SiGe HBT double quadrature downconverter with poly phase filters.

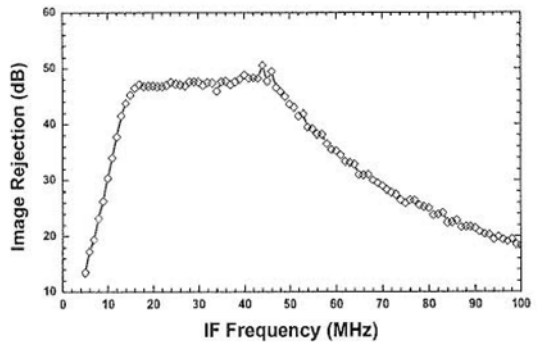


Figure 10 Image rejection ratios as a function of IF frequency for the SiGe HBT double quadrature downconverter with poly phase filters.

## IV. Conclusion

A fully integrated SiGe double quadrature Gilbert downconversion mixer with polyphase filters has been demonstrated for the first time in this paper to the best of our knowledge. A high image rejection double quadrature Gilbert downconverter with polyphase filters in the SiGe HBT technology has been achieved because GaAs has accurate thin film resistors and the low parasitic semi-insulating substrate. The fabricated SiGe HBT double quadrature Gilbert downconversion mixer with polyphase filters has 1 dB conversion gain, $IP_{1dB}$= -19 dBm and $IIP_3$= -9 dBm at 5.2 GHz. The image rejection ratio is better than 47 dB when LO=5.17 GHz and IF is in the range of 15 MHz to 45 MHz.

## Acknowledgement

This work was supported by the National Science Council of Republic of China under contract NSC 93-2219-E-009-026, by the Ministry of Education under contract 89-E-FA06-2-4 and by Ministry of Economic Affairs under contract number 92-EC-17-A-05-S1-020.

## References

[1] F. Behbahani, Y. Kishigami, J. Leete, and A. Abidi, "CMOS Mixers and Polyphase Filters for Large Image Rejection," IEEE Journal of solid-state circuits, VOL. 36, NO. 6, JUNE 2001.

[2] J. Crols and M. Steyaert, "Fully Integrated 900 MHz CMOS Double Quadrature Downconverter," Proc. ISSCC, Session 8.1, San Francisco, Feb. 1995.

[3] J. Crols and M. Steyaert, "A Single-Chip 900 MHz CMOS Receiver Front-End with a High Performance Low-IF Topology," IEEE J. of Solid-State Circuits, vol. 30, no. 12, pp. 1483-1492, Dec. 1995.

[4] M. Steyaert, M. Borremans, J. Janssens, B. D. Muer, N. Itoh, J. Craninckx, J. Crols, E. Morifuji, H. S. Momose and W. Sansen, "A single-chip CMOS transceiver for DCS-1800 wireless communications" Proc. ISSCC, San Francisco, Feb. 1998.

# A Fully Integrated 5.2 GHz SiGe HBT Upconversion Micromixer Using Lumped Balun and LC Current Combiner

Tzung-Han Wu, Chinchun Meng, Tse-Hung Wu and Guo-Wei Huang*

Department of Communication Engineering, National Chiao Tung University, Hsin-Chu, Taiwan, R.O.C.
*National Nano Device Laboratories, Hsin-Chu, Taiwan, R.O.C.

*Abstract* — **A small and compact 5.2 GHz upconversion Gilbert micromixer using 0.35 μm SiGe HBT technology is demonstrated in this paper. The upconversion micromixer has a broadband matched single-ended IF input port. A lumped-element rat-race hybrid is inserted in the LO input stage to maintain LO phase accuracy. A passive LC current combiner is used to convert the micromixer differential output into a single-ended output and double the output current. Thus, the IF port, LO port and RF port of the upconverter are single-ended, and the stand-along upconverter is suitable for hybrid RF system applications. The fully matched high linearity micromixer has the conversion gain of –1 dB, $OP_{1dB}$ of –10 dBm, $OIP_3$ of 6 dBm when input IF=300 MHz, LO=4.9 GHz and output RF=5.2 GHz. The IF input return loss is better than 10 dB for frequencies up to 20 GHz while the RF output return loss is better than 13.5 dB for frequencies up to 20 GHz. The supply voltage is 3.3 V, the current consumption is 11.5 mA, and the die size is 0.98x0.83 mm² with 6 integrated on-chip inductors.**

*Index Terms* — **Upconverters, Gilbert mixers, LC current combiners, lumped elements, rat-race hybrids.**

## I. INTRODUCTION

The double balanced Gilbert mixer [1] has been widely used in RFIC design for its compact size and excellent port-to-port isolation property. A fully integrated Gilbert upconversion micromixer with single-ended IF port, LO port and RF port is demonstrated at 5.2 GHz using 0.35 μm SiGe HBT technology. The single-ended upconverter here still maintains the truly balanced operation of the double balanced mixer. In addition, a stand-along single-ended upconverter is suitable for hybrid RF system applications. The circuit schematic is shown in Fig. 1. The upconversion micromixer [2]-[5] shown in figure 1 consists of a single-to-differential IF stage, a LO Gilbert mixer core, an RF output LC current combiner [6]-[8] with Darlington output buffer, and an on-chip lumped rat-race hybrid in the LO stage [9]-[11]. The micromixer input transconductance stage can turn the unbalanced IF input signal into differential currents needed by the Gilbert mixer core and provide wideband impedance matching.

A miniature lumped-element rat-race hybrid is integrated into the micromixer to achieve a balanced LO signals for the LO port of the upconverter. The integrated lumped rat-race hybrid provides excellent phase accuracy. When the integrated lumped-element rat-race hybrid is used to generate differential LO signals, it does not require any other extra off-chip trimming method to maintain balanced LO signals by using phase shifters for phase accuracy and rotary attenuators for magnitude balance. The lumped rat-race hybrid input stage generates balanced LO input signals, and the conversion gain and port-to-port isolations are maintained. Thus, a lumped-element rat-race hybrid consisting of inductors $L_3$ to $L_6$, capacitors $C_2$ to $C_8$, and a 50-ohm resistor is incorporated into this circuit to generate balanced LO input signals.

A passive LC current combiner is located at the output of the Gilbert mixer core to perform the differential-to-single conversion and double the output current at the resonant frequency. The output node taking from the LC current combiner behaves as a high impedance current source. Hence, a Darlington pair works as a voltage buffer to achieve a low impedance RF output port. Therefore, the conversion gain is maintained and the output impedance matching is achieved at the same time.

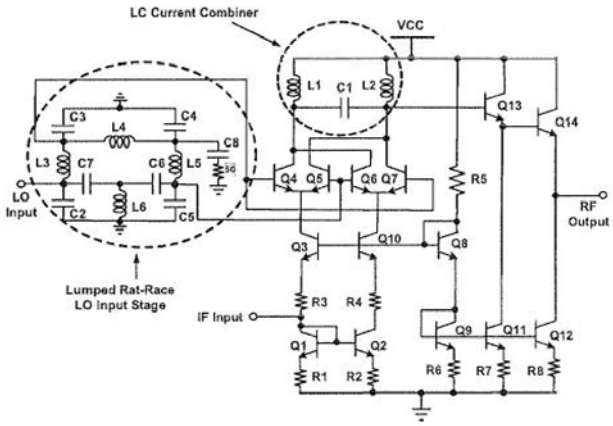


Fig. 1. Schematic of the fully integrated upconversion micromixer using lumped balun and LC current combiner.

The fully integrated 5.2GHz SiGe HBT upconversion micromixer with the LC passive current combiner in the RF output stage and the on-chip lumped-element rat-race in the LO stage has conversion gain of –1 dB, $OP_{1dB}$ of -10 dBm, $OIP_3$ of 6 dBm and 39 dB LO-RF isolation when input IF=0.3 GHz, LO=4.9 GHz and RF=5.2 GHz. The IF input return loss is better than 10 dB for frequencies up to 20 GHz while RF output return loss is better than 13.5 dB

0-7803-8846-1/05/$20.00 (C) 2005 IEEE

for frequencies up to 20 GHz. The supply voltage is 3.3V, and the current consumption is 11.5mA.

## II. Circuit Design

The photograph of the fabricated circuit is shown in Fig. 2. The total chip area is 0.98 x 0.83 $mm^2$ and there are six on-chip inductors. The SiGe HBT device used in this work has the following properties: $BV_{CEO}$=2.5V, and peak $F_t$ around 67 GHz. The emitter length of HBT is 5.1 μm with a non-self-aligned and single-poly-emitter device technology.

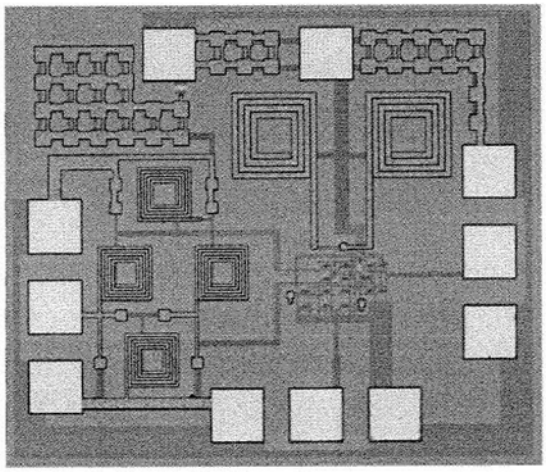

Fig. 2. Photograph of the fully integrated upconversion micromixer using lumped balun and LC current combiner.

For the IF input stage in Fig. 1, the common base stage, $Q_3$, has the equal but out of phase transconductance gain as the common emitter stage, $Q_2$, at the same bias currents. Thus, the differential currents needed by the Gilbert cell can be obtained by connecting $Q_1$ and $Q_2$ as a current mirror pair. The frequency response of the common emitter stage is improved by lowering the impedance seen at the base of $Q_2$. Thus, a micromixer input stage has a very good frequency response.

Generally speaking, an active current combiner (current mirror) limits the swing of the output signal and the performance of an active current mirror degrades very seriously for high frequency applications. Therefore, a passive LC current combiner is used as loads instead of using active current mirror as combining circuitry. In addition, the passive current combiner doubles the output current at the resonant frequency $\omega_0$, here

$$\omega_0 = \sqrt{\frac{1}{2L_1C_1}}.$$

Because the LC current combiner only consists of passive elements such as inductors and capacitors, there is an advantage that a circuit using the LC current combiner as the loading network has good linearity than the one using the active current mirror. Thus, an integrated passive LC current combiner at 5.2 GHz is designed in this work. The LC current combiner consists of two rectangular on-chip inductors as shown in the die photograph. On the other hand, a Darlington transistor pair consisting of transistor $Q_{13}$ and $Q_{14}$ is used to convert the output node of upconverter from a high impedance current source into a low impedance voltage source in order to maintain the conversion gain.

As shown in Fig. 1, the LO port of the Gilbert cell ($Q_4$, $Q_5$, $Q_6$ and $Q_7$) is connecting to a lumped-element rat-race hybrid. The rat-race hybrid is used to transform the unbalanced single-ended LO signal into balanced differential LO signals. For a stand-alone mixer, it is better to integrate the rat-race hybrid in the IC process because the lumped rat-race hybrid in the IC process has the ability to generate truly balanced signal. Since modern IC technology can precisely fabricate active devices and passive elements in the scale of several micrometers, thus the error due to process variation shall be in the order of several micrometers. The on-chip lumped-element rat-race hybrid also facilitates RF on-wafer measurement. In the RF measurement environment, there are usually many cables and adaptors for connecting probes and instruments. Generally speaking, most imbalances of input signals are usually caused by off-chip connecting components such as cables and couplers in the on-wafer RF measurement if an external rat-race hybrid is used. The phase error caused by cable bending is also a problem. A small bending of the cables may cause a serious phase imbalance between signals. Therefore, a most straightforward solution to this problem is to integrate the 180-degree hybrid network into the chip. In other words, the error in signal path lengths can be reduced from the orders of millimeters to micrometers by using IC technologies and thus phase imbalanced is improved dramatically.

## III. Experimental Result And Discussion

The 5.2 GHz upconversion micromixer with the integrated LC current combiner and the integrated lumped-element hybrid LO stage also facilitates on-wafer RF measurement. As shown in Fig. 2, the input GSG IF port is on the bottom side of the die while the output GSG RF port is on the right. LO GSG signal port is on the left, and the DC pads are on the top. The RF on-wafer measurement is simple because IF, LO and RF ports of this upconverter are single-ended.

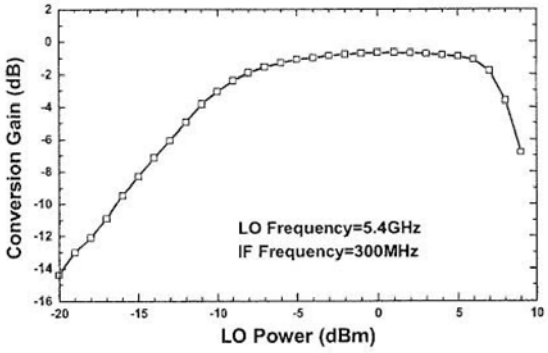


Fig. 3. Conversion gain vs. LO power of the fully integrated upconversion micromixer using lumped balun and LC current combiner.

The supply voltage is 3.3 V and the current consumption is 11.5 mA. The measured conversion gains as a function of LO power is shown in Fig. 3. As shown in Fig. 3, the peak conversion gain is –1dB when LO power changes from –6 to 5 dBm. In other words, the required LO power is small and there exists a wide range of LO power for optimum conversion gain.

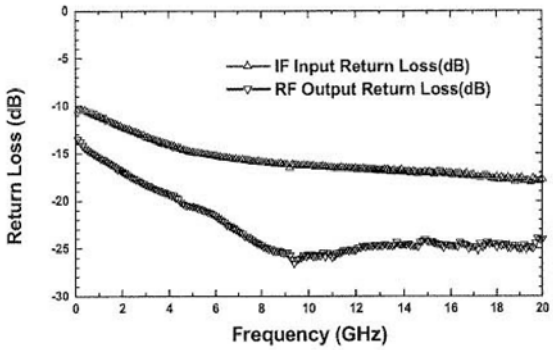


Fig. 4. IF port input return loss and RF port output return loss of the fully integrated upconversion micromixer using lumped balun and LC current combiner.

Fig. 4 shows the return loss of both IF and RF port. The RF output return loss is better than 13.5 dB from 0.1 GHz up to 20 GHz. A micromixer has a wide input matching bandwidth and the IF input return loss is better than 10 dB for frequencies up to 20 GHz as shown in Fig. 4. The power performance of the upconverter is shown in the Fig. 5. Experimental results show that the $OP_{1dB}$ is –10 dBm and the $OIP_3$ is 6 dBm. The high linearity property of the upconversion micromixer should directly come from using a passive LC current combiner as loading elements. Measured LO to RF isolation is 39 dB for 4.9 GHz LO input frequency. The high isolation property results from a truly balanced operation of a Gilbert micromixer with the output LC current combiner. The measured data shows that LO-IF isolation is 37dB.

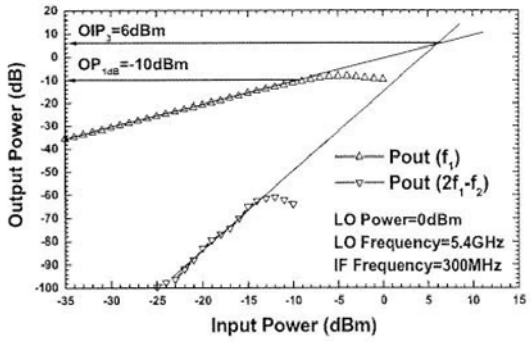


Fig. 5. Power performance of the fully integrated upconversion micromixer using lumped balun and LC current combiner.

## IV. Conclusion

A truly balanced Gilbert upconversion micromixer with the integrated LC current combiner and the integrated lumped-element hybrid is demonstrated using 0.35 μm SiGe HBT technology. The integrated lumped-element rat-race hybrid is used to convert the single-ended LO input signal into balanced differential signals. The upconvertion micromixer with single-ended IF, LO and RF ports is practical as a stand-alone mixer building block in the RF transmitter system. The fully matched integrated SiGe HBT upconverter has conversion gain of –1 dB, $OP_{1dB}$ of -10 dBm, $OIP_3$ of 6 dBm when input IF=0.3 GHz and thus output RF=5.2 GHz. The experimental results reveal that the upconvertion micromixer has good linearity by using the passive LC current combiner as the loading network. The IF input return loss is better than 10 dB for frequencies up to 20 GHz while RF output return loss is better than 13.5dB for output frequencies up to 20 GHz.

## Acknowledgement

The authors would like to thank National Chip Implementation Center (CIC) for technical support. This work was supported by the National Science Council of Republic of China under contract NSC 93-2752-E-009-003-PAE, NSC 93-2219-E-009-026 and by the Ministry of Economic Affairs under contract number 93-EC-17-A-05-S1-020.

## References

[1] B. Gilbert, "A precise four-quadrant multiplier with subnanosecond response," IEEE J. Solid-State Circuits, Vol. sc-3 No.4, pp. 365-373, Dec. 1968.

[2] B. Gilbert, "The MICROMIXER: A highly linear variant of the Gilbert mixer using a bisymmetric Class-AB input stage," IEEE J. Solid-State Circuits, Vol. 32, pp. 1412-1423, Sept. 1997.
[3] J. Durec, "An integrated silicon bipolar receiver subsystem for 900 MHz ISM band applications," IEEE J. of Solid-State Circuits, Vol. 33, No. 9, pp. 1352-1372, Sept. 1998.
[4] C. C. Meng, S. S. Lu, M. H. Chiang and H. C. Chen, "DC to 8 GHz 11dB gain Gilbert micromixer using GaInp/GaAs HBT technology," Electronic Letters, Vol. 39, No. 8, pp. 637-638, April 2003.
[5] Chinchun Meng, Tzung-Han Wu, Tse-Hung Wu and Guo-Wei Huang, "A 5.2GHz 16dB gain CMFB Gilbert downconversion mixer using 0.35um deep trench isolation SiGe BiCMOS technology," Digest, IEEE 2004 MTT-S, pp. 975-978.
[6] A. K. Wong, S. H. Lee and M. G. Wong, "Current combiner enhances active mixer performance," Microwave and RF, pp. 156-165, March 1994.
[7] Philips semiconductor, Plilips RF/Wireless communications data hand book, 1996.
[8] C. C. Meng, S. K. Hsu, A. S. Peng, S. Y. Wen and G. W. Huang, "A fully integrated 5.2GHz GaInP/GaAs HBT upconversion micromixer with output LC current combiner and oscillator," Digest, IEEE 2003 MTT-S, pp. A205-A208.
[9] S. J. Parisi, "180° lumped elements hybrid," IEEE MTT-S International Microwave Symposium Digest, Vol. 3, pp. 1243-1246, June 1989.
[10] A. P. Freundorfer and C. Falt, "A Ka-band GaInP/GaAs HBT Double Balanced Upconvert Mixer using Lumped Element Balun" IEEE MTT-S International Microwave Symposium Digest, Vol. 2, pp. 17-21, June 1996.
[11] I. Sakagami, M. Tahara, Y. Hao, and Y. Iwata, "Simplified lumped-element rat-race for a mobile receiver," 14th IEEE Proceedings on Personal, Indoor and Mobile Radio Communications, Vol. 3, pp. 2465-2469, Sept. 2003.

LETTER Special Section on Analog Circuit and Device Technologies

# A 5.7 GHz Gilbert Upconversion Mixer with an LC Current Combiner Output Using 0.35 $\mu$m SiGe HBT Technology

**Tzung-Han WU**[†], **Chinchun MENG**[†a)], **Tse-Hung WU**[†], *and* **Guo-Wei HUANG**[††], *Nonmembers*

**SUMMARY** This paper demonstrates a small compact 5.7 GHz upconversion Gilbert micromixer using 0.35 $\mu$m SiGe HBT technology. A micromixer has a broadband matched single-ended input port. A passive LC current combiner is used to convert micromixer differential output into a single-ended output and doubles the output current for single-ended-input and single-ended-output applications. Thus, a truly balanced operation of a Gilbert upconversion mixer with a single-ended input and a single-ended output is achieved in this paper. The fully matched upconversion micromixer has conversion gain of −4 dB, $OP_{1\,dB}$ of −9 dBm and $OIP_3$ of 4 dBm when input $IF$=0.3 GHz, $LO$=5.4 GHz and output $RF$=5.7 GHz. The IF input return loss is better than 18 dB for frequencies up to 20 GHz while RF output return loss is 25 dB at 5.7 GHz. The supply voltage is 3.3 V and the current consumption is 4.6 mA. The die size is 0.9 × 0.9 mm$^2$ with 3 integrated on-chip inductors.

***key words:*** *SiGe, HBT, Gilbert mixer*

## 1. Introduction

A fully matched and truly balanced Gilbert upconversion micromixer with a single-ended input and a single-ended output is demonstrated at 5.7 GHz in this paper by using a 0.35 $\mu$m SiGe HBT technology. The circuit schematic is illustrated in Fig. 1. A Gilbert micromixer [1] is used to transform the unbalanced single-ended input signal to the balanced differential signal. In addition, an LC output current combiner combines the differential output into a single-ended output.

A double balanced Gilbert mixer has been widely used in RF IC design because of the excellent port-to-port isolation property. The excellent performance in IF (RF) and LO port isolation is fundamentally achieved by separating IF (RF) and LO feeding ports in a Gilbert upconversion (downconversion) mixer. If the IF (RF) and LO signals that feed the Gilbert upconversion (downconversion) mixer are balanced, the IF-RF (RF-IF) and LO-RF (LO-IF) port-to-port isolation will be very high. Of course, the fact should be observed if the output signals are taken differentially. The transistor $Q_1$ and $Q_2$ basically form a current mirror and can be operated at very high frequencies. The common-base-biased transistor $Q_3$ and common-emitter-biased transistor $Q_2$ provide 180 degree out of phase transconductance gain when $Q_1$ and $Q_2$ are connected as a current mirror [2], [3]. Thus, the input stage in a micromixer can easily generate balanced RF signals and achieve broadband input impedance matching simultaneously. On the other hand, a traditional Gilbert mixer has an emitter coupled pair input stage and needs a current source to increase the common mode rejection ratio. Unfortunately, the common mode rejection provided by the biased current source in a conventional Gilbert mixer deteriorates rapidly at high frequencies and thus reduces the port-to-port isolation.

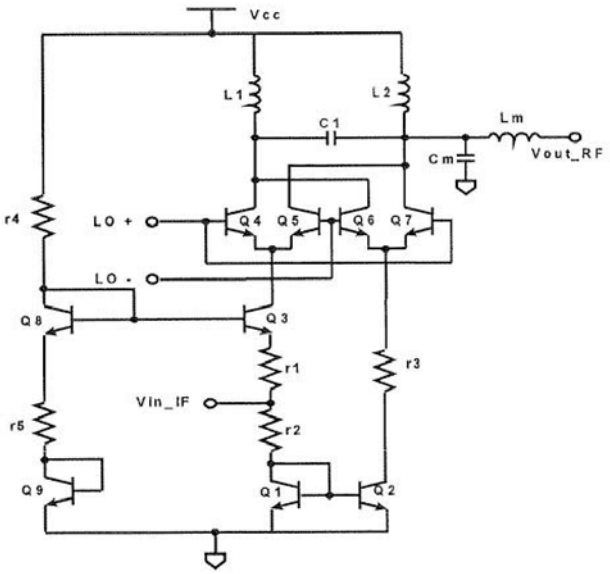


**Fig. 1** Schematic of an upconversion micromixer with an integrated LC current combiner and a low-pass LC matching output.

The upconversion mixer consists of a passive LC current combiner as the output stage. An LC current combiner is capable of doubling the output current and converts the differential output into a single-ended output [4], [5]. The LO input signal is generated by a broadband 180° coupler to maintain balanced LO signals. A low-pass LC network is used here for impedance matching. Thus, a truly balanced operation of a Gilbert upconversion micromixer with a single-ended input and a single-ended output is achieved in this paper.

The fully integrated SiGe HBT upconversion micromixer with a single-ended passive combiner output has conversion gain of −4 dB, $OP_{1\,dB}$ of −9 dBm, and $OIP_3$ of 4 dBm when input $IF$=0.3 GHz, $LO$=5.4 GHz and

Manuscript received October 23, 2004.
Manuscript revised January 8, 2005.

[†]The authors are with the Department of Communication Engineering, National Chiao Tung University, Hsinchu 300, Taiwan, R.O.C.
[††]The author is with National Nano Device Laboratories, Hsinchu 300, Taiwan, R.O.C.
a) E-mail: ccmeng@mail.nctu.edu.tw

DOI: 10.1093/ietele/e88–c.6.1267

$RF$=5.7 GHz. The IF input return loss is better than 18 dB for frequencies up to 20 GHz while RF output return loss is 25 dB at 5.7 GHz RF output frequency. The supply voltage is 3.3 V and the current consumption is 4.6 mA.

## 2. Circuit Design

The photograph of the fabricated circuit is illustrated in Fig. 2. The die size is $0.9 \times 0.9\,\mathrm{mm}^2$ and contains three on-chip inductors. The SiGe HBT device used in this work has $BV_{ceo}$=3.8 V, and peak $F_t$ around 49 GHz. The transistor emitter length is 9.9 $\mu$m with a non-self-aligned single-poly-emitter 0.35 $\mu$m SiGe HBT technology. The common-base-biased transistor $Q_3$ and common-emitter-biased transistor $Q_2$ provide 180 degree out of phase transconductance gain when $Q_1$ and $Q_2$ are connected as a current mirror. The common-base-configured transistor $Q_3$ possesses good frequency response while the speed of common-emitter-configured $Q_2$ is improved drastically by adding a low impedance diode-connected $Q_1$ at the input of common-emitter-configured $Q_2$. The input resistance equals to $(\frac{1}{g_{m3}} + r1) \| (r2 + \frac{1}{g_{m2}})$. This configuration achieves broadband impedance matching.

The Gilbert mixer core consists of transistors $Q_4$, $Q_5$, $Q_6$ and $Q_7$. The current combiner doubles the output current at the resonant frequency, $\omega_0 = \sqrt{\frac{1}{2L_1C_1}}$. A passive LC current combiner is used as loads instead of using a pair of active loads or resistors as combining circuitry. It is because the active current combiner limits the output signal swing and its performance unfortunately degrades very seriously for high frequency applications. Thus, an integrated passive LC current combiner at 5.7 GHz is designed in this paper.

In order to determine the effectiveness of the LC current combiner, a simulation with respect to current combining for the circuit in Fig. 1 is performed and shown in Fig. 3. There are two simulated output currents in Fig. 3. One current comes from one of the differential outputs of the Gilbert mixer core and equals to the summation of collector currents of transistor $Q_5$ and $Q_7$. The other one is the output current of the LC current combiner. The current combiner functions well because, as shown in Fig. 3, the output current from the LC current combiner is about two times of the current from one of the differential outputs of the Gilbert mixer core.

The design flow of a current combiner is described in three steps as follows:

Step 1: Decide the value of resonant frequency of the LC passive combiner.
Step 2: Choose the inductor as large as possible but make sure the inductor still functions as an effective inductor at the operating frequency. The unwanted parasitic capacitance of an on-chip inductor sets the practical upper frequency limit for an inductor to be effective. The larger the inductor is, the lower the upper frequency limit is. Thus, there exists a maximum inductor at a given operating frequency. A simple equivalent circuit model of the effective inductor consists of an inductance $L$ in series with a parasitic resistor $R_S$. Or, equivalently, the same value inductance $L$ in parallel with a parasitic resistor $R_P$. A large value inductor results in higher inductance $L$ and higher $R_P$. Thus, a large effective inductor can maintain the high conversion gain in Fig. 1 because of the associated high $R_P$. Once the maximum inductor is chosen and then the capacitance is determined by the resonant frequency.
Step 3: Design a proper LC low-pass filter that transforms output impedance to 50 Ω. At the mean time, the previous choosing inductor of the current combiner would have influence on the impedance transformation. In this procedure, we must check the inductance and redesign current combiner if necessary. There are three rectangular on chip inductors (two 2.4 nH and one 0.6 nH) in the die photograph of Fig. 2.

A low-pass LC network consisting of inductor $L_m$ and capacitor $C_m$ is used to improve the output matching as illustrated in Fig. 1. According to the design flow, the LC current combiner and the LC low pass network are designed to form a band-pass matching network and the designed center frequency is located at 5.7 GHz.

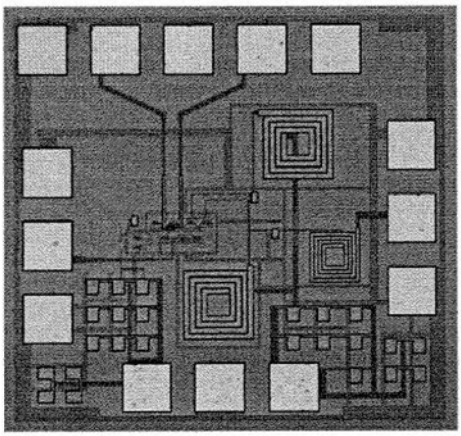

**Fig. 2** Photograph of the upconversion micromixer with an integrated output LC current combiner.

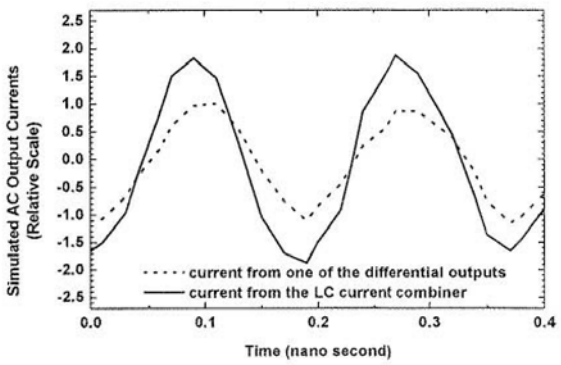


**Fig. 3** Simulated AC output currents. One current comes from one of the differential outputs of the Gilbert mixer core, the other one is the output current of the LC current combiner.

## 3. Measurement Results

Figure 2 shows the fabricated 5.7 GHz upconversion micromixer. The single-ended input and single-ended output configuration is convenient for on-wafer measurements. As shown in the photograph, The GSG IF input port is on the left side of the chip while GSG RF output port is on the right side. The GSGSG LO differential input pad is on the top side while the DC pads are on the bottom side. There are many small rectangular capacitors around the bottom side of the chip. These are bypassing or DC chocking capacitors. Because of the foundry process fabrication limitations, they should be implemented as capacitor arrays instead of one larger capacitor.

Figure 4 shows the measured conversion gain as a function of LO power. The peak conversion gain is −4 dB when LO power is 3 dBm as illustrated in Fig. 4. Figure 4 shows that conversion gain increases monotonically from −6 dB to −4 dB when LO power changes from −10 dBm to 3 dBm.

The Gilbert mixer core in Fig. 1 consists of emitter-coupled differential pairs. Only a small twist voltage in the range of several times of thermal voltage is needed to have current commutation in the emitter-coupled differential pairs. Therefore, the IF current commutation starts with small LO power of −10 dBm and thus the conversion gain can be maintained for a wide range of LO power as shown in Fig. 4.

Figure 5 shows that the RF output return loss is 25 dB at 5.7 GHz. Figure 5 also indicates that the LC current combiner functions very well. In our design, the operating output frequency is 5.7 GHz and the measurement results show that the output return loss has a notch exactly at 5.7 GHz. The exact output matching directly comes from the LC current combiner and LC low-pass filter. On the other hand, a micromixer has a wide bandwidth impedance matching and the IF input return loss is better than 18 dB for frequencies up to 20 GHz as shown in Fig. 4. We can assure that the input resistive matching indeed works perfectly based on the experimental data. The measured conversion gain as a function of IF frequency is illustrated in Fig. 5 and the conversion gain peaks around 0.3 GHz as expected because of the effectiveness of the LC current combiner. The LC current combiner filters signal around 5.7 GHz and the output current signal is doubled around 5.7 GHz. The LC current combiner is compact and very useful in an upconversion mixer design. As illustrated in Fig. 5 and Fig. 6, the output return loss and conversion gain versus IF frequency measurement results support the effectiveness of our LC current combiner design.

Power performance of the fabricated upconverter is shown in Fig. 7. Experimental result shows that the $OP_{1\,dB}$ is −9 dBm and the $OIP_3$ is 4 dBm.

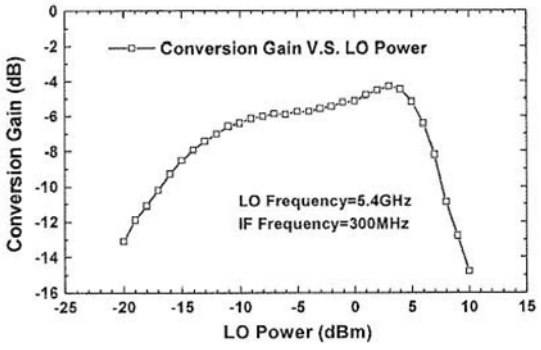


**Fig. 4** Conversion gain vs. LO power measurement of the upconversion micromixer with an integrated output LC current combiner.

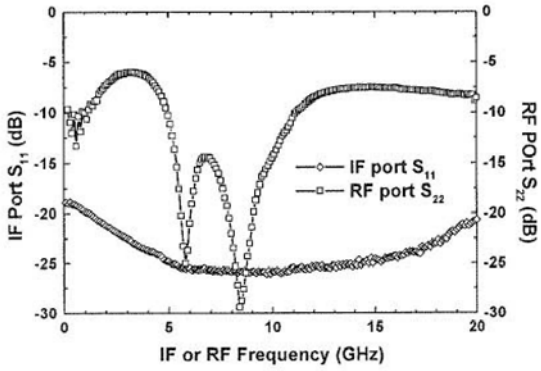


**Fig. 5** IF port input return loss and RF port output return loss of the upconversion micromixer with an integrated output LC current combiner.

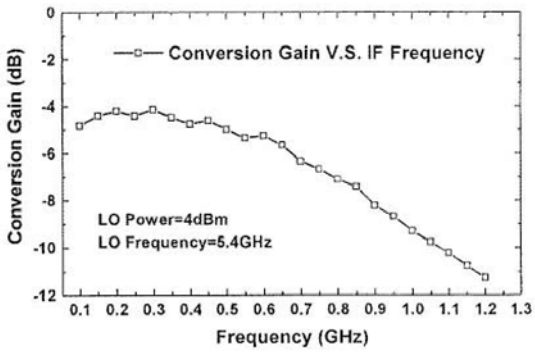


**Fig. 6** Conversion gain as a function of IF frequencies of the upconversion micromixer with an integrated output LC current combiner.

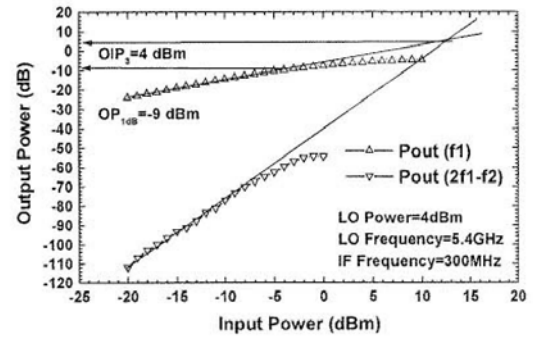


**Fig. 7** Power performance of the upconversion micromixer with an integrated output LC current combiner.

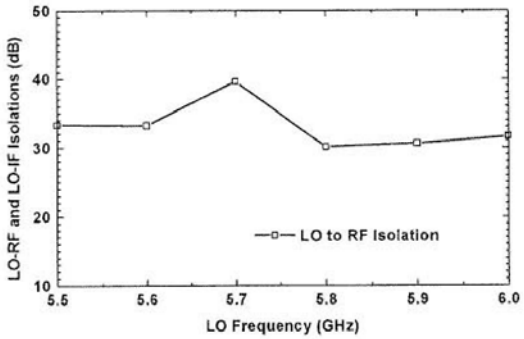


**Fig. 8** Measured LO-RF isolations of the upconversion micromixer with an integrated output LC current combiner.

The measured LO-RF isolation is shown in Fig. 8. The LO to RF isolation is 40 dB and at its best when LO frequency=5.7 GHz. This high isolation comes from the truly balanced operation of the mixer at the current-combining frequency.

## 4. Discussion and Conclusion

An upconversion micromixer is demonstrated in this paper. It has a single-to-differential input stage with a passive LC current combiner converting mixer differential output into a single-ended output. The fully matched and fully integrated SiGe HBT upconverter has conversion gain of −4 dB, OP1 dB of −9 dBm, and $OIP_3$ of 4 dBm when input $IF$=0.3 GHz and the output RF frequency equal to 5.7 GHz. The IF input return loss is better than 18 dB for frequencies up to 20 GHz while RF output return loss is 25 dB at 5.7 GHz output frequency. The die size is $0.9 \times 0.9\,mm^2$ with three on-chip rectangular inductors. The supply voltage is 3.3 V and the current consumption is only 4.6 mA.

## Acknowledgments

The authors would like to thank National Chip Implementation Center (CIC) for technical support. This work was supported by the National Science Council of Republic of China under contract NSC 93-2752-E-009-003-PAE, NSC 93-2219-E-009-026 and by the Ministry of Economic Affairs under contract number 93-EC-17-A-05-S1-020.

### References

[1] B. Gilbert, "The MICROMIXER: A highly linear variant of the Gilbert mixer using a bisymmetric class-AB input stage," IEEE J. Solid-State Circuits, vol.32, no.9, pp.1412–1423, Sept. 1997.

[2] J. Durec, "An integrated silicon bipolar receiver subsystem for 900 MHz ISM band applications," IEEE J. Solid-State Circuits, vol.33, no.9, pp.1352–1372, Sept. 1998.

[3] J. Durec and E. Main, "A linear class AB single-ended to differential transconverter suitable for RF circuits," IEEE MTT-S Dig., pp.1071–1074, 1996.

[4] A.K. Wong, S.H. Lee, and M.G. Wong, "Current combiner enhances active mixer performance," Microwave and RF, pp.156–165, March 1994.

[5] Philips Semiconductor, Philips RF/Wireless Communications Data Handbook, 1996.

# 2004 年亞太微波會議

孟慶宗
國立交通大學電信工程學系

(一)參加會議經過:

2004年亞太微波會議由印度舉行，地點在新德里的Ashok 飯店。會期自民國九十三年十二月十五日至十八日。此亞洲最大的微波會議每年召開一次，有來自各國近千人的科學家及研究員參與討論。在該會議中，中華民國所發表的論文數目名列前茅。討論主題有製程技術、射頻積體電路、微波電路模型、光通訊電路及天線等。而吾人的專長乃在主動元件及其電路，所發表的論文為有關GaInP/GaAs HBT的結構萃取方法，此論文引起不少人的興趣及重視。經過這幾天的切磋，大家都有所得。

(二)與會心得:

此會議有近千人參加，研討範圍廣泛，包含元件技術、射頻積體電路、光通訊電路、天線及微波電路模型，以不同場地同時進行。很明顯的，無線通訊已是一整合科技，以台灣所發表的論文程度與數量來看，國內微波的研究已達世界水準，而目前國科會也大力推動射頻 IC 研究，更能為我國科研形成面的結合，為業界培育新人才，使我國於無線通信領域大放異彩。

(三)建議:

此會議吸引各國研究人員參與，與他們討論切磋，可學到許多各公司或學校研究機構的詳細技術，並能激發創新的研究題材，希望國科會能夠大力資助國內研究人員參加此類會議。

(四)結論:

一. Solid-state device and circuit 佔了 12 個 sessions，明顯地有其重要性。

二. 此會乃是一結交無線通信技術人士的重要場合。

(五)攜回資料:

2004 APMC CD-ROM

# GaInP/GaAs HBT Device Structure Determination by DC Measurements on a Two-emitter HBT Device and High Frequency Measurements

C. C. Meng and B. C. Tsou*

Department of Communication Engineering, National Chiao Tung University, Taiwan, R.O.C.
Tel:886-3-5131379, fax:886-3-5736952, email:ccmeng@mail.nctu.edu.tw
*Department of Electrical Engineering, National Chung-Hsing University, Taichung, Taiwn, R. O. C.

***Abstract* — A method to monitor the GaInP/GaAs HBT device structure including ledge thickness is demonstrated in this paper. The base thickness and base doping density are obtained through base transit time and base sheet resistance measurements while the base transit time is measured through the cut-off frequency measurements at various bias points. A large size HBT device with two emitters is used to measure the ledge thickness. Emitter doping profile and collector doping profile can be obtained by the large size HBT device through C-V measurement. An FATFET device formed by two emitters as drain and source terminals and the interconnect metal as the Schotty gate on the ledge between two emitters is used to measure the ledge thickness.**

## I. INTRODUCTION

The HBT (Heterjunction Bipolar Transistor) structure strongly affects HBT's high frequency characteristics and reliability. It is desirable to confirm the layer structure and ledge thickness after the device has been fabricated. It has become especially important in today's foundry business model because normally the device structure is proprietary to the foundry company and will not be released to the circuit designer. On the other hand, it is advantageous for a circuit design company to make sure the device quality from lot-to-lot and wafer-to-wafer. Furthermore, it is necessary to fine tune the device structure and choose the right process if a better circuit performance is needed. In this paper, a method is established to find the device structure including ledge thickness for GaInP/GaAs HBT devices. Ledge thickness is an important parameter for reliability concern. The ledge thinning process in an HBT is not precisely controlled. Normally, a thicker-than-needed emitter is designed and a selective etching is used to remove the emitter cap for the emitter mesa. A wet etching dipping is used to thin down the emitter ledge to a totally depleted condition. The ledge thinning by chemically wet etching is somewhat uncontrollable. In some case, a thin emitter is designed such that, after the emitter cap is removed, the remaining ledge is already depleted. A quick wet etching dip is used to expose the fresh InGaP surface. In any case, a way to monitor the final ledge thickness is important to guarantee the device reliability. The method needs a special two-emitter large size HBT for ledge thickness measurement. The base thickness and doping density are obtained through base transit time and base sheet resistance measurements. The base transit time is obtained through S parameter measurement at various bias points. The cut-off frequencies at various collector current and collector voltage can be used to remove the effect of base-collector transit time and emitter charge time to obtain base transit time. A standard transmission line measurement is used to obtain the base sheet resistance. Thus, base thickness and base doping density can be obtained from base transit time and base sheet resistance. A large size HBT device with two emitters is developed in this paper to measure the ledge thickness, emitter and collector doping profiles. Emitter doping profile and collector doping profile can be obtained by the large size HBT device through C-V measurement. An FATFET device formed by two emitters as drain and source terminals and the interconnect metal as Schotty gate on the ledge between two emitters is used to measure the ledge thickness. The resulting measurement fits well with the material data.

## II. DEVICE STRUCTURE CHARACTERIZATION METHOD

A large size two-emitter HBT device is designed as shown in figure 1. A GaInP/GaAs HBT has a heavily doped base, thus a conventional C-V measurement can be used to obtain the emitter and collector doping profiles. The doping profiles for emitter and collector are illustrated in figure 2 and figure 3, respectively. Emitter doping is $3x10^{17}/cm^3$ and 0.067 μm thickness. Collector is $2x10^{16}/cm^3$ and 0.6 μm thickness. The ledge is strongly related to the device reliability. A fully depleted ledge prevents injected electron minority carriers from recombining at the exposed surface by inverting the band diagram at the surface. An FATFET device formed by two emitters as drain and source terminals and the interconnect metal as Schotty gate on the ledge between two emitters as illustrated in figure 1 is used to measure the ledge thickness. The C-V measurements in figure 4 reveal an unusually high doping starting at 0.051μm depth from the Schottky barrier surface. The measured unusually high doping density at this depth is caused by the heavily doped p type base. Thus, the C-V measurement can be

used to probe the ledge thickness even through the exact doping of the ledge can not be obtained.

A 2.4X3X2 HBT device is used to perform the high frequency S parameter measurement. The corresponding I-V curve is illustrated in figure 5. Forward Gummel plot and reversed Gummel plot are also illustrated in figure 5. The absence of the conduction band discontinuity in GaInP/GaAs interface can be evident by the fact that the Cummel plot for collector current overlays the reverse Gummel plot for reverse collector current. The almost zero conduction band discontinuity means that the GaInP material is an ordered structure instead of the disorder structure. An order GaInP emiiter has demonstrated a good reliability and thus the method here can also used to check the material quality.

S parameters are measured at various bias points and the cut-off frequency as a function of collector current and collector voltage is illustrated in figure 7. A Kirk effect is observed at high current. The emitter-collector charging time is the reciprocal of the cut-off radian frequency and is decomposed into emitter charging time, base transit time, base-collector transit time and collector charging time as follows.

$$\tau_{ec} = \frac{1}{2\pi f_t} = \frac{C_{je} + C_{jc}}{\frac{I_c}{V_t}} + \tau_B + \frac{X_{dep}}{2V_s} + \left(R_E + R_C\right) \cdot C_{jc}$$

It will be evident that the collector charging time is negligible. Thus, a plot of emitter-collector charging time as a function of the reciprocal of collector current as shown in figure 8 can be used to extrapolate the sum of base-transit time and base-collector transit time time. The base-collector transit time is a function of the base-collector voltage through the formula below.

$$\frac{qN_D X_{dep}^2}{2\varepsilon_s} = V_{CB} + V_{bi}$$

The base-emitter voltage is 1.4 Volt for the range of collector currents interested. Thus, a mapping between depletion width and base-collector voltage is obtain through C-V measurement. The sum of base transit and base-collector transit time can be ploted as a function of the depletion width to extrapolate the base-transit time. The base transit time is related to the base thickness by the formula below. The base layer sheet resistance can be obtained through the transmission line measurement. The sheet resistance is from a four point probe measurement.
The sheet resistance is related to the base doping density and base thickness by the formula below.

$$\tau_B = \frac{X_B^2}{2.43\mu_n V_T} = 2.334 \times 10^{-12}(s)$$

$$R_{SH} = \frac{1}{qN_B\mu_p X_B} = 159.35(\Omega)$$

The minority mobility and the majority mobility are related to the base doping density by the formula below.

$$\mu_n = \text{minority} \Rightarrow \mu_n = 8300\left(1 + \frac{N_B}{3.98\times10^{15} + \frac{N_B}{641}}\right)^{-\frac{1}{3}}$$

$$\mu_p = \text{majority} \Rightarrow \mu_p = \frac{380}{\left[1 + \left(3.17\times10^{-17}\right)\cdot N_B\right]^{0.266}}$$

Thus, by solving both equations, the base doping and thickness are.

$$N_B = 6.755 \times 10^{19}\left(cm^{-3}\right)$$

$$X_B = 1175\left(\overset{\circ}{A}\right)$$

The whole HBT structure together with ledge thickness is thus obtained.

## III. CONCLUSION

The HBT (Heterjunction Bipolar Transistor ) structure strongly affects HBT's high frequency characteristics and reliability. It is advantageous for a circuit design company to make sure the device quality from lot-to-lot and wafer-to-wafer. A method to determine the HBT device structure and material quality by DC and RF measurements have been developed in this paper. The whole HBT structure together with ledge thickness is very useful to fine tune the device structure and choose the right process if a better circuit performance is needed.


## ACKNOWLEDGEMENT

This work was supported by the National Science Council of Republic of China under contract NSC 92-2219-E-009-023 and by the Ministry of Education under contract 89-E-FA06-2-4.


## REFERENCE


[1] W. Liu, "Handbook of III-V heterojunction bipolar transistors", John Wily & Sons.

[2] W. Liu, T. Henderson, E. Beam III and S. K. Fan, "Electron saturation velocity in $Ga_{0.5}In_{0.5}P$ measured in a GaInP/GaAs/GaInP double-heterojunction bipolar transistor", Electronics Letters, Vol. 29, No. 21, p1885-1887, October 1993.

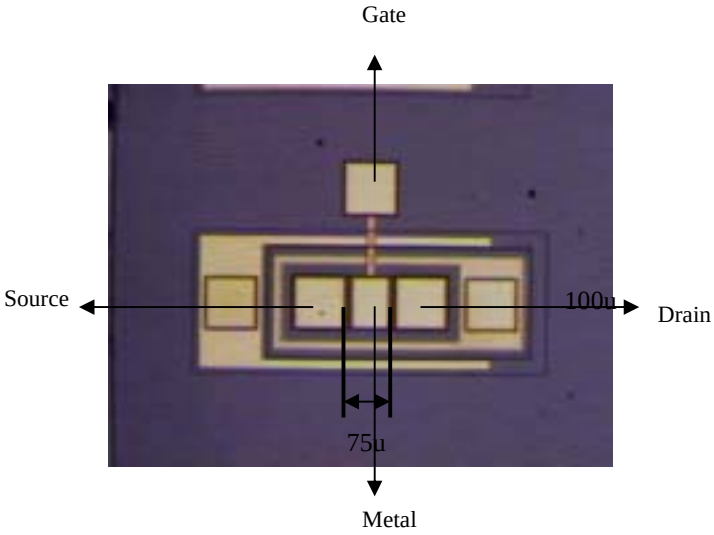


Figure 1. The two-emitter HBT device for measuring ledge thickness, emitter doping profile and collector doping profile. The two emitters are used as drain and source while the interconnect metal is used as the gate metal for the ledge between two emitters.

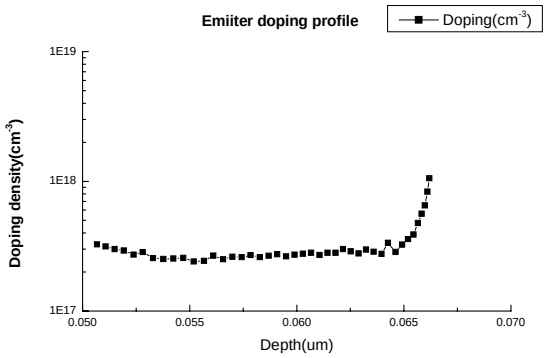


Figure 2. The emitter doping profile obtained through C-V measurement.

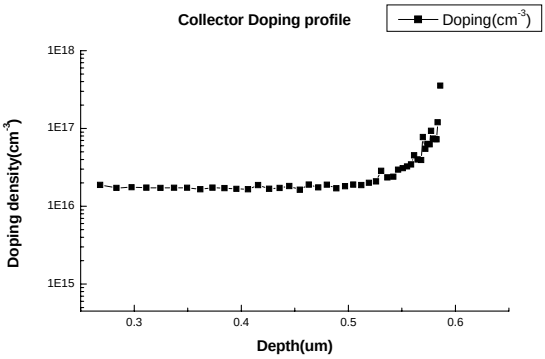


Figure 3. The collector doping profile obtained through C-V measurement.

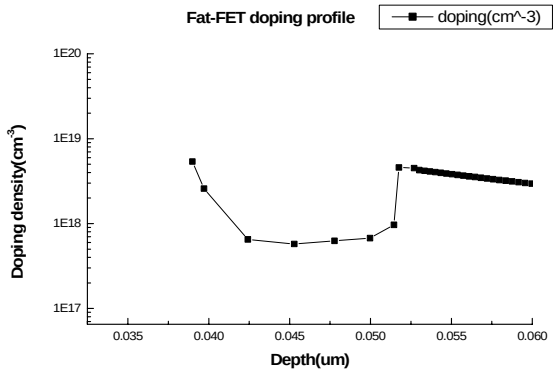


Figure 4. The ledge thickness measurement.

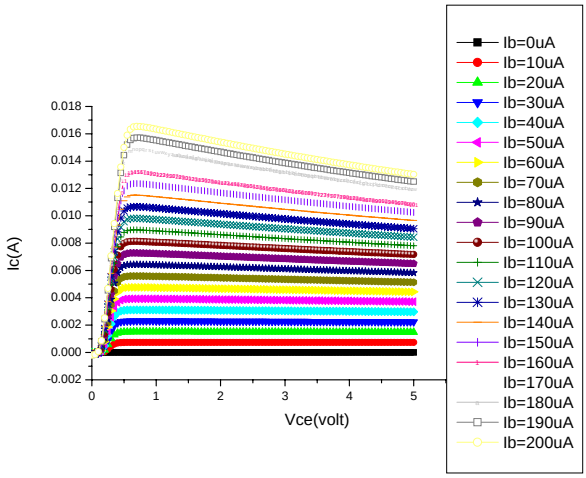


Figure 5. I-V curve of 2.4X3X2 HBT device.

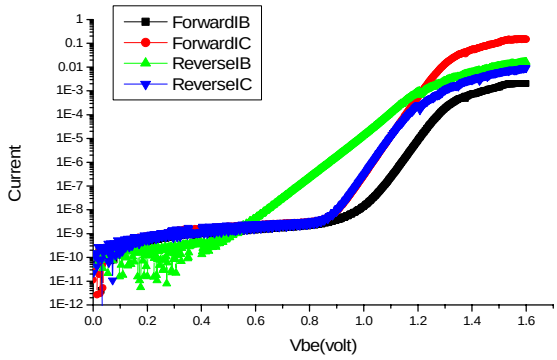


Figure 6. GUmmel plot of 2.4X3X2 HBT device.

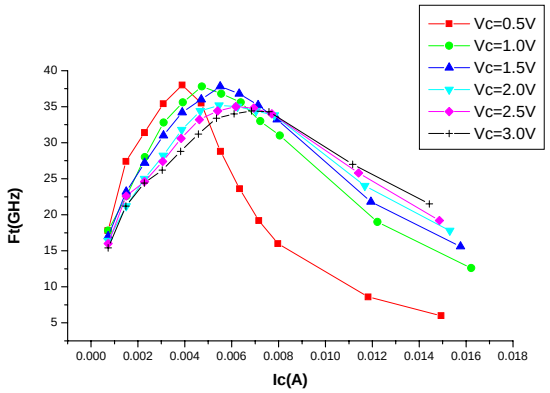


Figure 7. Cutoff frequency as a funvtion of collector current with collector-emitter voltage as a parameter

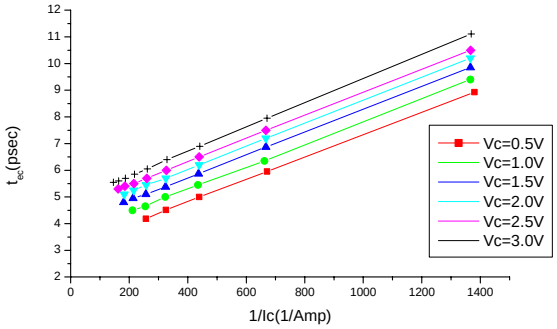


Figure 8. A plot of emitter-collector charging time as a function of the reciprocal of collector current. The plot can be used to extrapolate the sum of base-transit time and base-collector transit time.

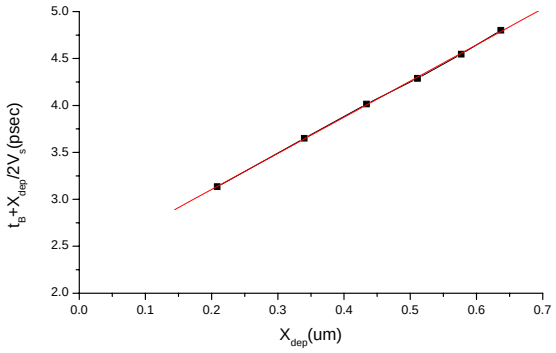


Figure 9. A plot of the sum of base-transit time and base-collector transit time as a function of the depeltion width. The plot can be used to extrapolate the base transit time.

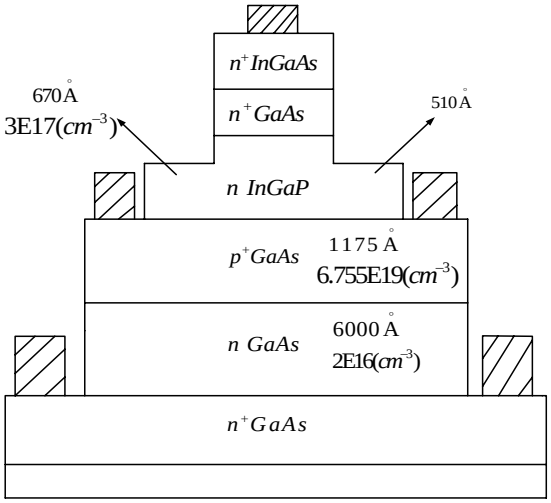


Figure 10. The HBT layer structure including ledge determined by the DC and RF measurements.